Preparation and Characterization of a Poly(β-hydroxyoctanoate) Latex Produced by *Pseudomonas oleovorans*

Alain Dufresne* and Eric Samain

Centre de Recherches sur les Macromolécules Végétales (CERMAV-CNRS), Université Joseph Fourier - BP 53, 38041 Grenoble Cedex 9, France

Received March 31, 1998; Revised Manuscript Received July 7, 1998

ABSTRACT: A latex of poly(β-hydroxyoctanoate) was obtained from *Pseudomonas oleovorans* grown at high cell density on sodium octanoate. A fermentation using a pH-stat control of octanoate concentration as well as the purification steps using sodium hypochlorite were described. It was observed that latex stabilization occurred spontaneously due to the persistence around the polymer granules of the murein sacculus, which envelopes the bacterial cell. Films were processed by casting and evaporating the polymeric aqueous suspension and were characterized by scanning electron microscopy, wide-angle X-ray scattering, dynamic mechanical analysis, and tensile tests. It was shown that the optimal conditions for the bacteria digestion correspond to a hypochlorite concentration between 21 and 26 mmol of NaOCl/g of biomass. These conditions enable latex stabilization and satisfactory mechanical properties of the resulting film.

Introduction

Polymer aqueous suspensions, or latices, have generated great interest due to their industrial applications as films, coatings, and composites as well as blends with other polymers. Indeed, it is well-known that emulsion polymerization can lead to materials easily processed, either by film casting techniques (water evaporation) or by freeze-drying followed by the classical extrusion process. As a matter of fact, different monomers can be statistically copolymerized to adjust the glass−rubber transition temperature at a given value.[1] More generally, it is also possible to mix different types of water suspensions including some polymer latices and organic or inorganic stabilized suspensions. Previous works performed in our laboratory deal with the processing and the characterization of nanocomposite materials with a synthetic polymeric latex as the matrix reinforced by cellulose whiskers or starch microcrystals.[2−5]

Poly(hydroxyalkanoates) (PHAs) are biopolymers stored by a wide variety of bacteria as an energy reserve.[6−8] They accumulate in intracellular inclusion bodies and are a carbon reserve and energy source for the bacteria.[7] PHAs are thermoplastic materials, and in contrast to synthetic polymers, they have the fundamental advantage of being renewable resources not dependent on the supply of petroleum.

Due to their natural origin, PHAs have an exceptional stereochemical regularity, which enables the polymer to crystallize.[9,10] The most common PHA is poly(β-hydroxybutyrate) (PHB), a highly crystalline and brittle thermoplastic. In contrast, the bacterium *Pseudomonas oleovorans* has the ability to grow on a variety of long chain fatty acids and to produce PHA containing a long pendant group in each repeat unit.[10−15] When the bacterium is grown on octanoic acid, the resulting polymer is a copolymer containing poly(β-hydroxyoctanoate) (PHO) and has the properties of a thermoplastic elastomer.[16−18]

* To whom correspondence should be addressed (e-mail: dufresne@cermav.cnrs.fr).

As an intracellular product, the separation of PHAs from the rest of the cell is a major factor in the economic feasibility of commercial production and in obtaining material of adequate quality to study their mechanical, physical, and chemical properties. Three major separation procedures of PHA from bacteria cells exist: solvent extraction, chemical digestion, and selective enzymolysis.[19] The first is the most commonly used technique and a number of solvent extraction processes have been developed to separate PHA from the biomass. These methods usually involve the use of a chlorinated solvent such as chloroform[20,21] and 1,2-dichloroethane,[22,23] azeotropic mixtures (e.g., 1,1,2-trichloroethane with water,[24] chloroform with either methanol, ethanol, acetone, or hexane[25]), acetic anhydride,[26] or cyclic carbonates (e.g., hot (120−150 °C) ethylene or 1,2-propylene carbonate).[27] The solution can, therefore, be cast to prepare films. Apart from being expensive, these methods generally involve handling large quantities of toxic, volatile solvent.

Methods of preparation of artificial granule suspensions of PHAs have been described in the literature by Horowitz et al.[28−31] and by Marchessault et al.[32] In both methods, PHA is extracted with chloroform and purified from the biomass. In other words, native PHA storage granules are first dissolved and the granular structure is recovered after specific treatments.

Compared to solvent extraction, the other two methods (chemical digestion and selective enzymolysis) consist of selective removal of non-PHA components and these methods can preserve the nascent state and the granular morphology of PHA, allowing more diverse applications than solvent-extracted PHA. They are, therefore, suitable for latex production. A procedure in which cells are ruptured by thermal treatment and the resultant debris is treated with an enzyme cocktail to solubilize all cell components apart from PHA was described in earlier studies.[33,34] The resulting PHA suspension was washed with an anionic surfactant (e.g., SDS assisted by EDTA) and concentrated.

Another separation procedure, using differential digestion with sodium hypochlorite to separate bacterial

S0024-9297(98)00508-7 CCC: $15.00
Published on Web 08/22/1998

Table 1. Characteristics of the Samples According to the Sodium Hypochlorite Content Used to Purify the Bacteria[a]

sample	mmol of NaOCl added/g of biomass	nitrogen content (%)	$10^{-3}\bar{M}_n$	$10^{-3}\bar{M}_n$	$\bar{M}_w/\bar{M}_n$	particle size (μm)
A	12.8	0.76	83	138	1.66	1.15
B	17.1	0.65	78	150	1.94	1.03
C	21.4	0.56	83	172	2.07	0.92
D	25.6	0.55	92	183	2.00	1.05
E		0.15	89	141	1.59	

[a] Sample E is used as a reference and corresponds to PHO purified from the biomass by chloroform extraction.

biomass from PHB, is described by Williamson and Wilkinson.[35] Although simple and effective, this method has been avoided because it has been reported to cause severe degradation of the PHB molecular weight.[36−38] However, operating conditions under which sodium hypochlorite could digest bacterial biomass without serious degradation of the PHB were optimized by balancing the ratio of hypochlorite to non-PHB biomass.[39−41]

The aim of the present paper is to develop a technique of obtaining a stable latex of PHO directly from the biomass without loss of the native granular structure. The granule suspension is characterized, as well as the films resulting from the coalescence of this polymer.

Experimental Section

Bacterial Strain and Growth Conditions. *P. oleovorans* (ATCC 29347) was grown on a mineral medium having the following composition: sodium octanoate (20 mM), NH_4Cl (0.15 g·L^{-1}), KH_2PO_4 (10 g·L^{-1}), $MgSO_4{\cdot}7H_2O$ (1 g·L^{-1}), trace mineral solution (10 mL/L). $MgSO_4$ was autoclaved separately. The trace mineral stock solution contained nitrilotriacetic acid (70 mM, pH 6.5), $FeSO_4{\cdot}7H_2O$ (5 g·L^{-1}), $MnCl_2{\cdot}4H_2O$ (0.85 g·L^{-1}), $CoCl_2{\cdot}6H_2O$ (0.14 g·L^{-1}), $CuCl_2{\cdot}2H_2O$ (0.085 g·L^{-1}), H_3BO_3 (0.17 g·L^{-1}), $ZnSO_4{\cdot}7H_2O$ (0.9 g·L^{-1}), and $Na_2MoO_4{\cdot}2H_2O$ (0.09 g·L^{-1}). In the preculture medium the NH_4Cl concentration was increased to 1 g·L^{-1}.

High cell density cultures were performed in a 10 L fermenter. The dissolved oxygen was maintained at 20% air saturation by automatically adjusting the stirrer speed and by manually increasing the air flow rate up to 420 L·h^{-1}. The pH was regulated at 6.85 by automatic addition of pure octanoic acid. The temperature was maintained at 30 °C. The initial culture volume was 6.5 L. The cultivation was started by the inoculation (2% vol/vol) of a preculture grown for 24 h. After 5 h of cultivation, two separate feeding solutions, one containing ammonium octanoate (1 M, pH 8.0) and the other one containing $MgSO_4{\cdot}7H_2O$ (25 g·L^{-1}) were connected to the fermenter. The initial feeding rate was 3.6 mL·h^{-1}. This rate was exponentially increased up to 36 mL·h^{-1} in 12 h (feeding phase 1) and then maintained at 36 mL·h^{-1} for 7 h (feeding phase 2). The feeding rate was then lowered down to 12 mL·h^{-1} and kept at this value for the last 24 h (feeding phase 3).

Bacterial growth was followed by measuring the increase in the optical density (OD) at 540 nm. In addition, the dry weight was determined from an aliquot of culture medium. Cells were recovered by centrifugation for 3 min at 12000*g*, rinsed in distilled water, centrifuged again, and dried at 70 °C until the weight remained constant. The relation between the OD and the cell dry weight was found to vary slightly from 0.22 to 0.19 g/unit of OD between the beginning and the end of the culture.

Digestion of Biomass by Hypochlorite. The culture was collected at the end of feeding phase 3 and was centrifuged 20 min at 12000*g*. The supernatant was discarded, and the cells were suspended at a concentration of 10 g·L^{-1} in distilled water. To purify the PHO, cell suspensions were treated with different amounts of sodium hypochlorite (Table 1). The concentrated hypochlorite solution (2.14 M) was slowly added to the cell suspensions to limit heating and to prevent the pH from rising above 10. The suspensions were then incubated for 2 h at 37 °C and centrifuged at 12000*g* for 30 min. PHO granules were washed with distilled water and finally resuspended in distilled water at a concentration of about 50 g·L^{-1}.

Film Processing. The PHO granule suspensions were purified by 15 h dialysis against distilled water. The air in the suspension was removed by vacuum prior to casting in a Teflon mold (2 × 7 mm). Films were obtained by storing the casting at 40 °C to allow water evaporation and particle coalescence.

As a reference system, PHO was purified by chloroform extraction as described elsewhere.[11] After solvent extraction, the PHO solution was cast in a Teflon mold (2 × 7 mm) and allowed to slowly evaporate at room temperature.

Microscopies. Scanning electron microscopy (SEM) was performed to investigate the morphology of the materials with a JEOL JSM-6100 instrument. The specimens were frozen under liquid nitrogen, then fractured, mounted, coated with gold on a JEOL JFC-1100E ion sputter coater, and observed. SEM micrographs were obtained using 7 kV secondary electrons.

Transmission electron microscopy (TEM) observations were achieved with a Philips CM200 electron microscope operating at 80 kV. *P. oleovorans* containing PHO granules were observed as thin sections prepared as follows. Samples were fixed at room temperature in a freshly prepared mixture of 0.3% glutaraldehyde and 2% paraformaldehyde in distilled water as described elsewhere.[42] After rinsing, bacterial cells were dehydrated through a progressive ethanol series up to 70%, then progressively infiltrated, embedded in LR White resin (hard mixture, TAAB), and finally polymerized 24 h at 50 °C. Resin-embedded bacteria were sectioned using ultramicrotomy and poststained with 2.5% aqueous uranyl acetate (2 min).

Elemental Analysis. Elemental analyses were performed by the Analysis Central Service of CNRS (Centre National de la Recherche Scientifique), Vernaison, France. The carbon, hydrogen, oxygen, and nitrogen contents of PHO films were determined as described elsewhere.[43]

Molecular Weight Measurements. Number average molecular weight, M_n, weight average molecular weight, M_w, and polydispersity index $\bar{M}_w/\bar{M}_n$ were determined by size exclusion chromatography (SEC) with a Waters apparatus (510 pump), using a set of four columns (Styragel HR0.5, HR1, HR2, and HR5). The mobile phase was tetrahydrofuran, with an eluent flow rate of 1.1 mL·min^{-1}. A refractive index detector (Waters 410) was used for detection. For calibration, polystyrene standard solutions were injected.

Sieve Analysis. Particle size and particle-size distributions of PHO granules were obtained from dynamic light scattering (quasi-elastic light scattering) with a Malvern Autosizer Lo-Ci instrument. The diluted polymer suspension was set in a cell and exposed to a monochromatic beam (λ = 670 nm). Particles shift under the Brownian motion and oscillate around an equilibrium position. Intensity fluctuations scattered at 90° are amplified and used to determine the diffusion coefficient. The particle mean diameter was calculated from the Stokes−Einstein equation. The values reported in this work are the average of at least five measurements. The distribution of the particle size was characterized by the variance. A latex was considered monodisperse if the variance was lower than 0.02, of narrow distribution if the variance was between 0.02 and 0.1, and of broad distribution if the variance was beyond 0.1.

X-ray Diffraction. Wide-angle X-ray scattering (WAXS) patterns of all materials were measured in reflection with a

diffractometer using a static detector (Siemens D500). Samples were mounted on a support and exposed for a period of 10 s for each angle of incidence using a Cu Kα1 X-ray source with a wavelength of 1.5406 Å operating at 40 kV and 20 mA. The angle of incidence was varied between 3° and 30° by steps of 0.04°. WAXS patterns were recorded at several time intervals after film formation to ensure perfect reliability of measurements and to detect any possible evolution of the material with time.

Dynamic Mechanical Analysis. Dynamic mechanical tests were carried out with a Rheometrics RSA2 spectrometer in the tensile mode. Test conditions were chosen in such a way that the measurements were in the linear viscoelasticity region (the maximum strain ϵ was around 10^{-4}). The specimen was a thin rectangular strip with dimensions of 30 × 3 × 1 mm. Measurements were performed in isochronal conditions at 1 Hz, and the temperature was varied between 200 and 380 K by steps of 3 K.

Tensile Tests. The nonlinear mechanical behavior was analyzed using an Instron 4301 testing machine in tensile mode, with a load cell of 100 N capacity. The specimen was a thin rectangular strip (~30 × 5 × 1 mm). Tensile tests were performed at a strain rate $\dot{\epsilon} = 1.7 \times 10^{-3}\ s^{-1}$ (cross-head speed = 1 mm/min) and at 25 °C. The true strain ϵ can be determined by $\epsilon = \ln(l/l_o)$, where l and l_o are the length during the test and the length at zero time, respectively. The stress σ was calculated by $\sigma = F/S$, where F is the applied load and S is the cross-sectional area. Stress versus strain curves were plotted and Young's modulus (E) was measured from the low strain region.

Ultimate mechanical properties were also characterized. The nominal ultimate stress, or nominal stress at break, $\sigma_{bn} = F_b/S_o$, as well as the true ultimate stress, $\sigma_b = F_b/S$, where F_b is the applied load at break, were reported for each tested sample. Ultimate elongation was characterized by the nominal ultimate strain, or nominal strain at break, $\epsilon_{bn} = \Delta l_b/l_o$, and by the true ultimate strain, $\epsilon_b = \ln[1 + (\Delta l_b/l_o)]$, where Δl_b is the elongation at break. The values reported are the average of at least five measurements.

Results and Discussion

PHA Production. *P. oleovorans* accumulates poly(3-hydroalkanoates) (PHAs) when its growth is limited by some essential nutrients (nitrogen, phosphate, magnesium) or oxygen and when it is cultivated in the presence of an excess of the carbon source. However, sodium octanoate inhibits growth at concentrations higher than 30 mM,[11] and this inhibition limits the initial substrate concentration that can be used in the starting media. To obtain high yields of PHA in high cell density cultures of *P. oleovorans*, our strategy was to limit growth by a continuous feeding of nitrogen (provided as ammonium octanoate) and to maintain the sodium octanoate at a non-growth-limiting concentration by automatically regulating the pH of the culture by pure octanoic acid. As octanoic acid is mainly present in the fermentation mixture as sodium octanoate (the initial concentration is 20 mM), the utilization of octanoic acid by the cells must result in an alkalanization of the medium. By regulating the pH with pure octanoic acid, the amount of octanoic acid consumed by the cells should theoretically be replaced and the sodium octanoate concentration should stay constant. However, this system can only work if there is no other interfering pH-modifying phenomena. For example, providing nitrogen as ammonium chloride would have resulted in an acidification of the medium due to the utilization of ammonia by the cells. This effect was prevented by supplying the nitrogen as ammonium octanoate. In this case the consumption of ammonia did not cause acidification since the counterion is released as octanoic acid and is used by the cells.

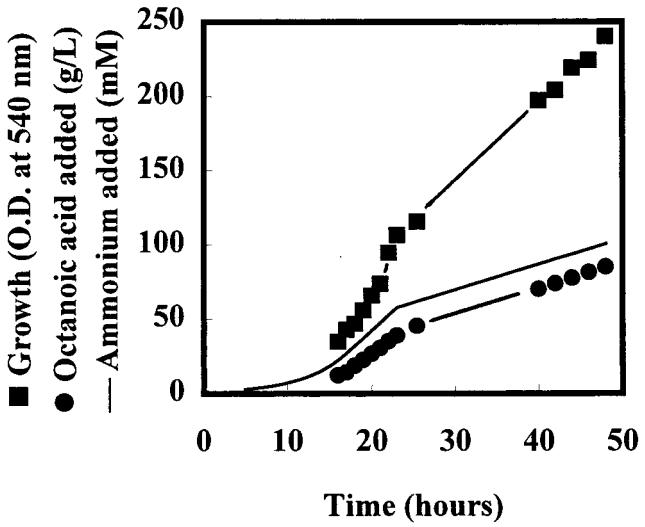

Figure 1. Growth of *P. oleovorans* in an ammonium-limited fed-batch culture with a pH-stat control of octanoate concentration: (■) growth; (●) octanoic acid added. The line corresponds to the cumulative amount of added ammonium octanoate.

After inoculation, the cells grew exponentially until complete exhaustion of the nitrogen source, which was initially added in the starting medium at a low concentration (2.8 mM). The cell growth was then nitrogen-limited but not carbon-limited, and the growth rate was controlled by the feeding of an ammonium octanoate solution. During the feeding phase 1, the ammonium octanoate input rate was exponentially increased (μ = 0.192) from 0.5 to 5.0 mmol·h^{-1}·L^{-1} resulting in an exponential growth up to an OD of 42 (Figure 1). To prevent oxygen limitation, the ammonium octanoate input rate was then kept constant at 5.0 mmol·h^{-1}·L^{-1} in the feeding phase 2. Despite this constant ammonium feeding rate, the rate of biomass formation continued to increase exponentially (μ = 0.067 h^{-1}), resulting in an increase in the oxygen demand. The rate of ammonium octanate input was then reduced to 1.3 mmol·h^{-1}·L^{-1} to avoid oxygen limitation (feeding phase 3) and the growth proceeded linearly for 24 h up to an OD of 240. The final cell dry weight was 47 g·L^{-1} with a PHA content of 55%. The total amount of octanoic acid consumed was 84 g·L^{-1}, of which 70 g·L^{-1} was supplied as pure octanoic acid by the pH regulation system and 14 g·L^{-1} was provided as ammonium salt by the continuous feeding.

***In Vivo* Polymer Granules Morphology.** The *in vivo* PHO inclusions morphology was observed by TEM. Figure 2 shows a thin section of *P. oleovorans* bacteria, prepared as described in the Experimental Section. Polymer inclusions with diameters of about 1 μm occurred as egg-shaped white gaps within the bacterial cell. PHO was actually removed from the bacteria during the thin section preparation step, and the resulting gaps were filled with the inclusion resin. Each cell contained generally a single particle, but two or three granules could coexist in the same cell. The size and number of polymer inclusions per bacterial cell depended on the organism used to produce PHA. For instance, *Ralstonia eutropha* cells contained typically 8−12 PHB granules with diameters ranging between 0.2 and 0.5 μm, which represented about 80% of the bacterium dry weigth.[29]

Digestion of Biomass by Sodium Hypochlorite. When biomass was treated with more than 25 mmol of

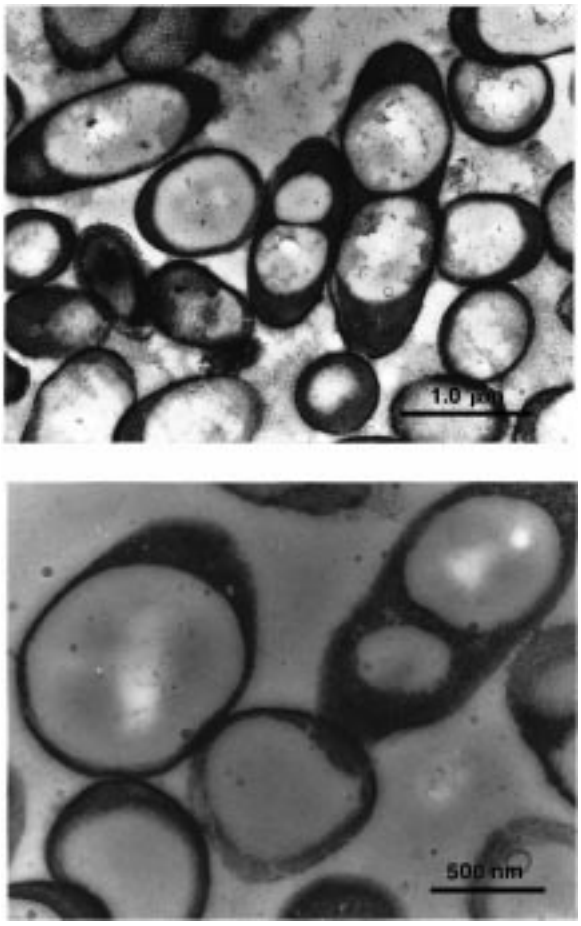

Figure 2. Transmission electron micrographs of a thin section of *P. oleovorans* showing PHO inclusion morphology.

NaOCl/g of biomass, a coalescence of PHA granules was observed during the purification process and most of the PHA was recovered as a gummy material. On the contrary, when the digestion was conducted with lower hypochlorite concentration, a stable suspension of granules was obtained. However, reduction of the hypochlorite concentration resulted in a decrease in the PHA purity as indicated by the increase in the nitrogen content (Table 1). This increase was especially marked for hypochlorite treatments lower than 20 mmol of NaOCl/g of biomass (samples A and B). However, whatever the sodium hypochlorite concentration may be, the nitrogen content was always higher than that for the solvent-extracted polymer (Table 1).

In the range of hypochlorite concentration tested, no significant change in the number average molecular weight ($\bar{M}_n$) was observed (see Table 1). In addition, $\bar{M}_n$ values were very close to those of samples purified with chloroform (Table 1). On the contrary, the hypochlorite treatment seemed to have caused an increase in the $\bar{M}_w$ value (Table 1). The weight average molecular weight increased continuously from 137 000 to 183 000 for samples A to D. This increase was also displayed by the asymmetric form of the peaks obtained in GPC experiments. Moreover, it is worthy to note that it was very difficult to dissolve samples C and D, which were obtained at higher hypochlorite content, prior to GPC experiments. These two materials tended to swell rather than dissolve.

It is noteworthy that the stabilization of PHO granules was obtained without any surfactant. An explanation of this unusual phenomenon could be the persistence of the murein sacculus, which envelopes the bacterial cell. The treatment of granule suspensions (3 $g \cdot L^{-1}$) with lysozyme (1 $g \cdot L^{-1}$) (which is known to specifically hydrolyze the murein sacculus) resulted in an immediate coalescence of PHA granules as observed by optical microscopy (Figure 3). Treatment with bovine serum albumine at the same concentration as lysozyme did not cause any coalescence. These results suggest that the coalescence of PHA granules was effectively preserved only by the murein sacculus, which has not been completely removed during the hypochlorite digestion.

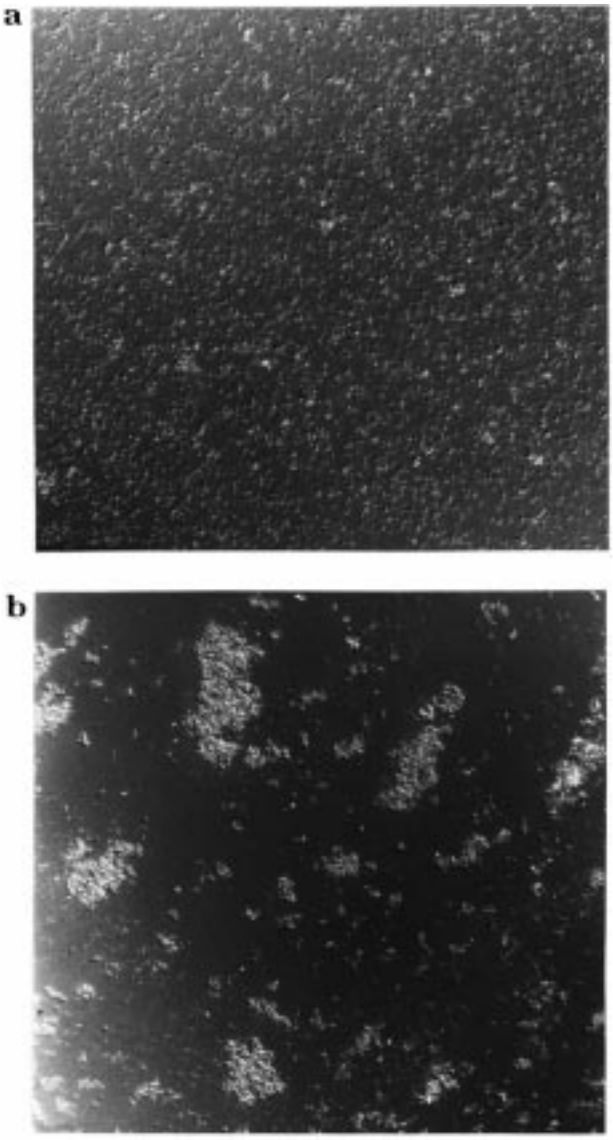

Figure 3. Optical micrograph (×40) showing (a) the stabilized latex B and (b) latex B immediately after treatment with lyzozyme. Photograph reduced to 72% for publication.

Polymer Granule Morphology in the Latex. Particle sizes of PHO granules extracted from the biomass by sodium hypochlorite treatment were obtained from dynamic light scattering measurements (Table 1). It was observed that the average particle diameter of PHO granules in the latex was around 1 μm, which corresponded to the in vivo inclusion dimension. Therefore, the sodium hypochlorite extraction treatment allowed the preservation of the native granular structure. The variance reached a maximum unity value regardless of the extraction conditions. This

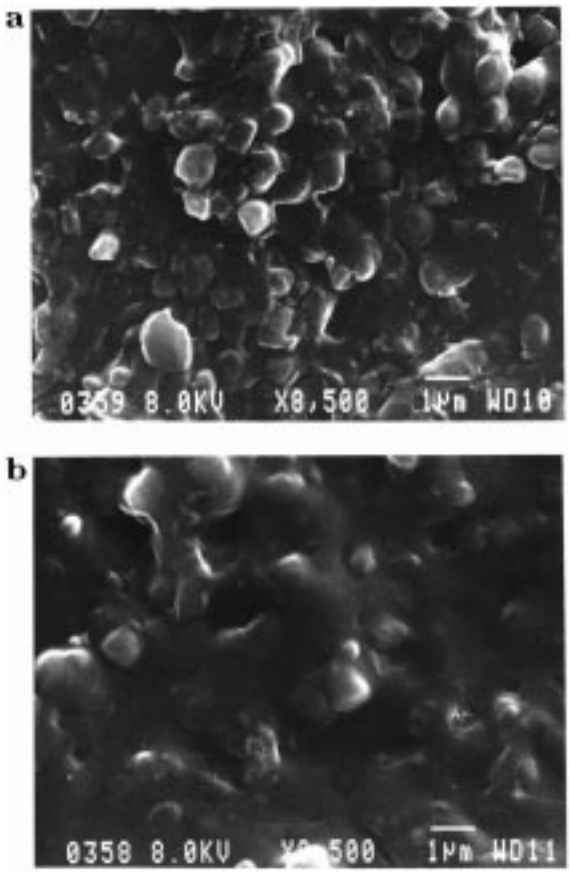

Figure 4. Scanning electron micrographs of freshly fractured surface PHO films: (a) sample A and (b) sample D.

result can be explained on one hand by the broad particle size distribution of the native granules (Figure 2) and on the other hand by their oval shape, which disturbed the variance of the measurement.

Morphological Characterization of Films. Examination of the surfaces of fractured films obtained from latices A and D clearly show that the fracture surface of film D (Figure 4b) was much smoother than that of film A (Figure 4a). Hence, film cohesion and film processing was better when higher sodium hypochlorite concentrations were used to purify the PHO granules. The coalescence of polymeric chains in sample A was probably hindered by the presence of a more intact murein sacculus. Indeed, low sodium hypochlorite concentrations were favorable for stabilizing the polymer suspension but prevented in turn the film formation by particle coalescence. However, it is worthy to note that film formation was obtained without any apparent problem at the macroscopic level, regardless of what the hypochlorite concentration was.

Wide-angle X-ray scattering (WAXS) was used to characterize PHO films obtained from latices purified either by sodium hypochlorite treatment or by chloroform extraction (Figure 5). The amorphous part of the polymer was characterized by a broad hump located around $2\theta = 20°$, whereas the crystalline zones display three diffraction peaks near 5, 20, and 22°. No significant difference was observed in the diffraction patterns of films A to D, which indicated that the amount of sodium hypochlorite used to purify PHO granules did not influence significantly the crystallinity of the material. Furthermore, the diffraction patterns of films obtained from latices extracted with sodium hypochlorite did not differ significantly from that corresponding to the film prepared by the solvent extraction procedure (film E). Hence, the extraction procedure did not disturb the crystallinity ratio and crystal structure.

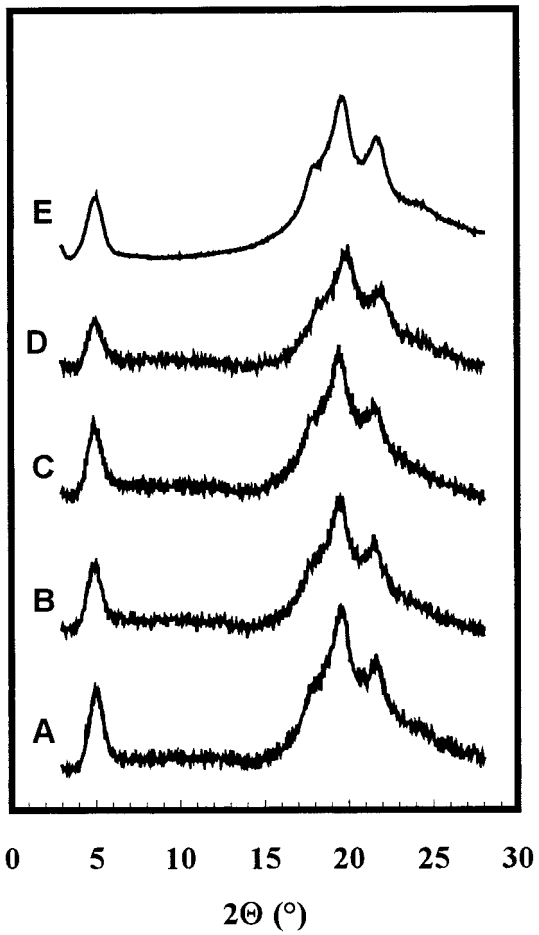

Figure 5. Wide-angle X-ray diffraction patterns for PHO films obtained from latices purified by sodium hypochlorite treatment (samples A to D) or chloroform extraction (sample E).

Dynamic Mechanical Analysis. The tensile dynamic mechanical behavior of PHO films obtained from the coalescence of polymer granules extracted by sodium hypochlorite digestion were compared to that of PHO films processed by solvent extraction and casting (Figure 6).

For low temperatures, it was difficult to observe any change in the modulus with variation in the extraction procedure. As it is well-known, the exact determination of the glassy modulus depends on the precise knowledge of the sample dimensions. In this case, at room temperature, the films were soft and it was very difficult to obtain a constant and precise thickness along these samples. Furthermore, the difference between the elastic modulus of the crystalline domains and that of the amorphous zones was not high enough to easily appreciate any change. To minimize this effect, the samples were frozen in liquid nitrogen prior to the experiments to accurately measure their dimensions. However, to be able to compare the effect of extraction procedure on the drop of the elastic tensile modulus, E' at 150 K was normalized at the average measured value (2 GPa) for all the samples.

At higher temperatures, a rapid decrease in the elastic tensile modulus (Figure 6a), by 1 or 2 decades, depending on the sample, was observed, corresponding

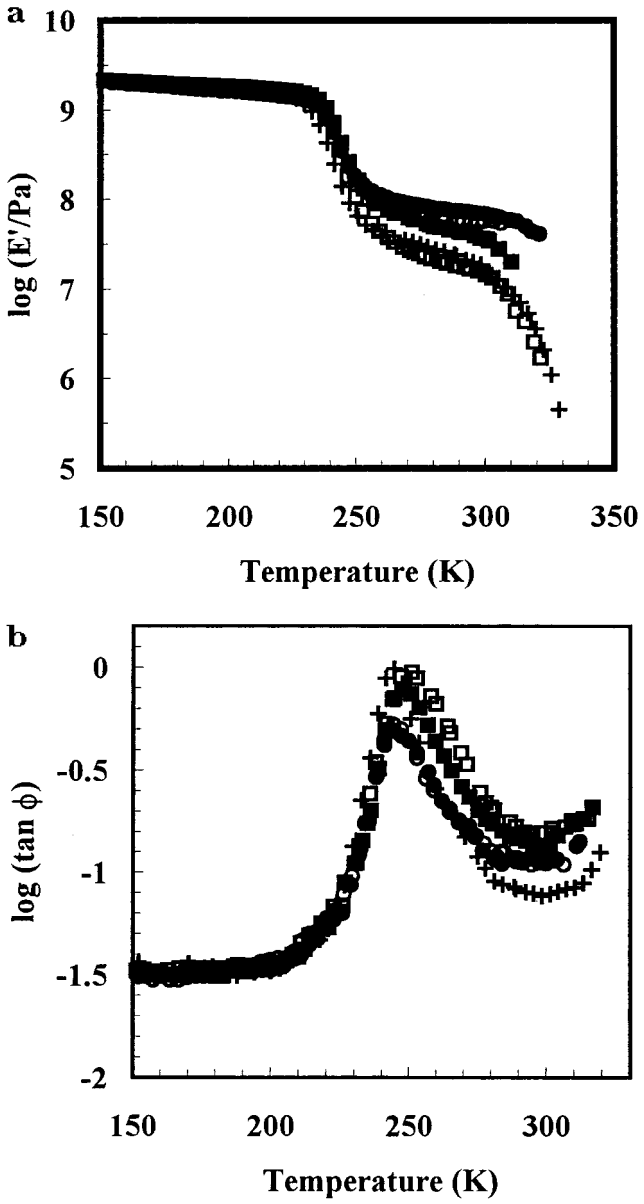

Figure 6. (a) Logarithm of the storage tensile modulus E' and (b) logarithm of the loss angle tangent tan ϕ versus temperature at 1 Hz for samples (●) A, (○) B, (■) C, (□) D, and (+) E.

to the glass−rubber transition. This modulus drop corresponds to an energy dissipation displayed in a relaxation process where tan ϕ passes through a maximum (Figure 6b). This relaxation process, labeled α, involves cooperative motions of long chain sequences.

The rubbery modulus is known to depend on the degree of crystallinity of the material. The crystalline regions of PHO act as physical cross-links for the elastomer. In this physically cross-linked system, the crystalline regions would also act as filler particles due to their finite size, which would increase the modulus substantially. Figure 7 shows the evolution of log(E'/Pa) as a function of temperature for different annealing treatments of sample A at room temperature after film formation. It was observed that the relaxed modulus increased with annealing time. After 2 weeks, the relaxed modulus did not change further. Curves displayed in Figure 6 were obtained at least 2 weeks after film formation to ensure perfect reliability of measurements.

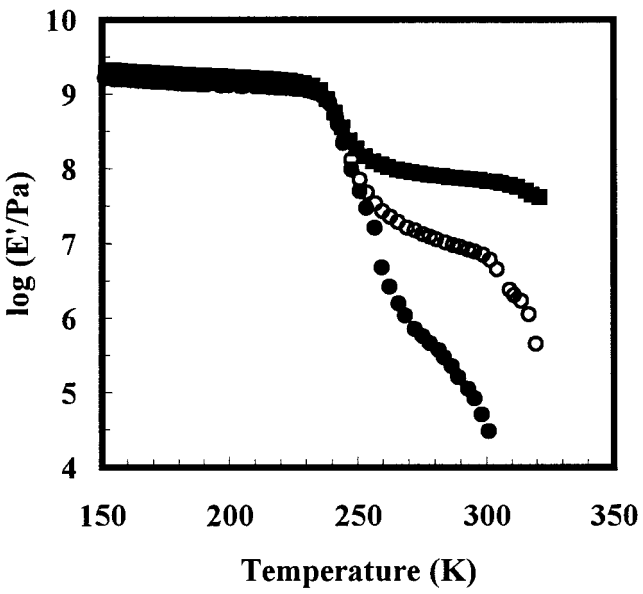

Figure 7. Logarithm of the storage tensile modulus E' versus temperature at 1 Hz for sample A after (●) 0, (○) 1, and (■) 2 weeks annealing times at room temperature after film formation.

Above T_g, the relaxed modulus increased as the sodium hypochlorite concentration decreased (Figure 6a). For instance, the rubbery modulus at T_g + 50 °C (∼285 K) of sample A is about 100 MPa, whereas it is 20 MPa for sample D. This phenomenon cannot be due to degree of crystallinity changes in the polymeric film with extraction conditions, because no change in the WAXS diffraction patterns were observed (Figure 5). It was probably mainly due to the murein sacculus, which reinforced the material as hard inclusions. The mechanical behavior of the chloroform extracted film (sample E) was similar to that of sample D, i.e., when the digestion was conducted with the higher hypochlorite concentration.

By comparison with the solvent extracted polymer (sample E), the modulus drop associated with T_g occurred at a higher temperature for samples A to D (Figure 6a). The temperature shift, of about 5 K, is slight but significant and could be due to remaining murein sacculus within the polymer. However, in the case of sodium hypochlorite extracted PHO, the T_g or T_α shift should depend on the murein sacculus content and, therefore, on the hypochlorite concentration. A possible explanation could be a change in the crystalline domain size with purification method, but it would result in a modification of the crystalline peaks width in WAXS patterns, which was not observed (Figure 5). Another explanation could be the existence of stronger intermolecular interactions in sodium hypochlorite extracted polymer compared to the solvent-purified one. These interactions could induce some constraints in the molecular mobility, which would result in a shift toward higher temperatures of T_g. These constraints could originate from specific interactions between remaining sodium hypochlorite and segments of PHO. It can be related to the $\bar{M}_w$ increase observed in GPC with hypochlorite concentration used to purify samples. This increase in $\bar{M}_w$ value could result from a slight and spontaneous cross-linking of PHO chains in the presence of hypochlorite sodium. This phenomenon could be related to the fact that samples C and D were difficult to solubilize in chloroform for GPC analysis.

Table 2. Mechanical Properties of PHO Films: Tensile Modulus, E, Nominal Ultimate Stress, σ_{bn}, True Ultimate Stress, σ_b, Nominal Ultimate Strain, ϵ_{bn}, and True Ultimate Strain, ϵ_b

sample	E (MPa)	σ_{bn} (MPa)	σ_b (MPa)	ϵ_{bn} (%)	ϵ_b (%)
C	32.8	1.3	1.4	8.3	8.0
D	6.0	1.7	9.6	405	159
E	13.1	6.5	43.4	555	186

The α relaxation process is characterized by its temperature position and also by its intensity, which mainly depends on the magnitude of the modulus drop and by its half-height width, which is representative of the size distribution of mobile entities participating in the relaxation process. The interesting feature in Figure 6b is the larger half-height width of the α relaxation process for samples C and D, compared with samples A, B, and E. It is observed that this increase is due to a peak broadening toward higher temperatures. Therefore, the size distribution of macromolecular chains involved in the main relaxation process in samples C and D was broader, and this phenomenon was due to the participation of higher molecular weight chains. This result is in good agreement with the GPC experiments and with the increase in the weight-average molecular weight observed with increasing sodium hypochlorite concentration.

High Strain Behavior. All results lead to the conclusion that murein sacculus remained after the hypochlorite treatment and stabilized the polymer suspension. Assuming this point, one wonders whether this remaining membrane affected the ultimate properties of PHO films. Tensile tests could provide an answer to this question, and the mechanical properties of PHO samples C, D, and E are reported in Table 2. The stress-strain curves (not depicted here) displayed behavior typical of thermoplastic elastomers. The tensile or Young's moduli reported in Table 2 are in agreement with storage tensile moduli measured at room temperature (Figure 6a). The tensile modulus observed with the film obtained from chloroform extraction (sample E, 13.1 MPa) agrees with what was reported in earlier studies. Gagnon et al.[17,44] reported tensile modulus values ranging from 2.5 to 9 MPa, depending on the crystallization temperature, for films prepared from PHO by melt blending the polymer in a glass casting dish. This modulus is lower than the one reported by Marchessault et al. (17 MPa),[45] but it is well-known that the tensile modulus greatly depends on the experimental conditions, such as strain rate and temperature. The highest value of Young's modulus was observed with sample C, as a consequence of the presence of the murein sacculus, as observed previously for the rubbery modulus in dynamic mechanical analysis.

The ultimate properties of PHO films are reported in Table 2. The nominal and true stresses and strains were calculated as described in the Experimental Section. PHO purified from the biomass by chloroform extraction (sample E) displayed a typical rubber-like behavior with a high strain at break (ϵ_{bn} > 500%). When biomass was treated with high hypochlorite concentration (sample D), a high elongation at break was also observed. However, ϵ_{bn} and ϵ_b values were lower than those for sample E. This decrease probably resulted from the lower purity of the polymer, and thus from the fact that the material became less extensible as the number of impurities increased. This phenomenon was much more pronounced for sample C, which displayed a dramatic decrease in the ultimate elongation. The nominal elongation at break showed a 400% decrease when the hypochlorite concentration decreased from 25 to 21 mmol of NaOCl/g of biomass. However, it is worthy to notice that for sample C, the breaking of the material occurred in a completely different manner. Samples D and E showed a continuous increase in stress until sudden fracture at a strain of about 400−500%. Sample C, however, reached a maximum stress at a strain of about 8% whereupon the sample began tearing slowly and the stress decreased. This peculiar behavior of sample C probably resulted from the presence of murein sacculus, which prevented the film formation by particle coalescence and restricted the molecular diffusion. This suggestion agrees with the SEM observation (Figure 4). The values of ϵ_{bn} and ϵ_b reported in Table 2 for sample C were assigned to the maximum load and therefore to the initiation of the fracture.

Conclusion

A latex of PHO was prepared using a chemical treatment by sodium hypochlorite. It was shown that the stabilization of the latex occurred spontaneously without any surfactant. This phenomenon was due to the persistence around the polymer granules of the murein sacculus, which envelope the bacterial cell *in vivo*. In contrast to what was observed in the literature with PHB, no significant degradation of the polymer was reported after the purification procedure. On the contrary, a surprising increase of the weight-average molecular weight, $\bar{M}_w$, was observed as the hypochlorite concentration used to purify PHO was increased. This increase was probably due to specific interactions between remaining sodium hypochlorite and PHO. These interactions could lead to a slight and spontaneous cross-linking of PHO in the presence of sodium hypochlorite. The optimal conditions for the bacteria digestion corresponded to a hypochlorite concentration between 21 and 26 mmol of NaOCl/g of biomass. The processing and characterization of natural nanocomposite materials with PHO latex as the matrix and polysaccharide fillers, like starch microcrystals, cellulose whiskers, and cellulose microfibrils were also investigated, and results will be published shortly.

Acknowledgment. The authors gratefully acknowledge Mr. L. Dumas for his help in film processing, Mr. Graillat for sieve analysis, Dr. M. Valière and Mrs. D. Mallarde for GPC experiments, Mrs. E. Hesse for her help in tensile tests, and Mrs. D. Dupeyre and Dr. K. Ruel for their help in SEM and TEM, respectively.

References and Notes

(1) Schlund, B.; Guillot, J.; Pichot, C. *Polymer* **1989**, *60*, 1883.
(2) Favier, V.; Canova, G. R.; Cavaillé, J. Y.; Chanzy, H.; Dufresne, A.; Gauthier, C. *Polym. Adv. Technol.* **1995**, *6*, 351.
(3) Helbert, W.; Cavaillé, J. Y.; Dufresne, A. *Polym. Compos.* **1996**, *17*, 4, 604.
(4) Dufresne, A.; Cavaillé, J. Y.; Helbert, W. *Macromolecules* **1996**, *29*, 7624.
(5) Dufresne, A.; Cavaillé, J. Y.; Helbert, W. *Polym. Compos.* **1997**, *18*, 2, 198.
(6) Dawes, E. A.; Senior, P. J. *Adv. Microbiol. Physiol.* **1973**, *10*, 135.
(7) Erson, A. J.; Dawes, E. A. *Microbiol. Rev.* **1990**, *54*, 4, 450.
(8) Doi, Y. In *Microbial Polyesters*; VCH Publishers: New York, 1990.
(9) Cornibert, J.; Marchessault, R. H. *J. Mol. Biol.* **1972**, *71*, 735.
(10) Preusting, H.; Nijenhuis, A.; Witholt, B. *Macromolecules* **1990**, *23*, 4220.

(11) Brandl, H.; Gross, R. A.; Lenz, R. W.; Fuller, R. C. *Appl. Environ. Microbiol.* **1988**, *54*, 1977.
(12) De Smet, M. J.; Eggink, G.; Witholt, B.; Kingma, J.; Wynberg, H. *J. Bacteriol.* **1988**, *154*, 870.
(13) Lageveen, R. G.; Huisman, G. W.; Preusting, H.; Ketelaar, P.; Eggink, G.; Witholt, B. *Appl. Environ. Microbiol.* **1988**, *54*, 2924.
(14) Gross, R. A.; DeMello, C.; Lenz, R. W.; Brandl, H.; Fuller, R. C. *Macromolecules* **1989**, *22*, 1106.
(15) Huisman, G. W.; DeLeeuw, O.; Eggink, G.; Witholt, B. *Appl. Environ. Microbiol.* **1989**, *55*, 1949.
(16) Gagnon, K. D.; Lenz, R. W.; Farris, R. J.; Fuller, R. C. *Rubber Chem. Technol.* **1992**, *65*, 4, 761.
(17) Gagnon, K. D.; Lenz, R. W.; Farris, R. J.; Fuller, R. C. *Macromolecules* **1992**, *25*, 3723.
(18) Gagnon, K. D.; Lenz, R. W.; Farris, R. J.; Fuller, R. C. *Polymer* **1994**, *35*, 20, 4358.
(19) Lauzier, C. A.; Monasterios, C. J.; Saracovan, I.; Marchessault, R. H.; Ramsay B. A. *Tappi J.* **1993**, *76*, 5, 71.
(20) Walker, J.; Whitton, J. R.; Alderson, B. Eur. Pat. Appl. 46,-017, 1982.
(21) Vanlautem, N.; Gilain, J. U.S. Pat. 4, 310,684, 1982.
(22) Barham, P. J.; Sealwood, A. Eur. Pat. Appl. 58,480, 1982.
(23) Holmes P. A.; Jones, E. Eur. Pat. Appl. 46,335, 1980.
(24) Vanlautem, N.; Gilain, J. U.S. Pat. 4,705,604, 1987.
(25) Stageman, J. F. U.S. Pat. 4,562,245, 1985.
(26) Schmidt, J.; Biederman, B.; Schmiechen, H. Ger. (East) Pat. DD 223,428, 1985.
(27) Lafferty, R. M.; Heinzle, E. U.S. Pat. 4,101,533, 1978.
(28) Horowitz, D. M.; Clauss, J.; Hunter, B. K.; Sanders J. K. M. *Nature* **1993**, *363*, 23.
(29) Horowitz, D. M.; Sanders J. K. M. *J. Am. Chem. Soc.* **1994**, *116*, 7, 2695.
(30) Horowitz, D. M.; Sanders J. K. M. *Polymer* **1994**, *35*, 23, 5079.
(31) Horowitz, D. M.; Sanders J. K. M. *Can. J. Microbiol.* **1995**, *41* (Suppl. 1), 115.
(32) Marchessault, R. H.; Morin, F. G.; Wong, S.; Saracovan, I. *Can. J. Microbiol.* **1995**, *41* (Suppl. 1), 138.
(33) de Koning, G. J. M.; Witholt, B. *Bioprocess Eng.* **1997**, *17*, 7.
(34) de Koning, G. J. M.; Kellerhals, M.; Van Meurs, C.; Witholt, B. *Bioprocess Eng.* **1997**, *17*, 15.
(35) Williamson, D. H.; Wilkinson, J. F. *J. Gen. Microbiol.* **1958**, *19*, 198.
(36) Alper, R.; Lundgren, D. G.; Marchessault, R. H.; Cote, W. A. *Biopolymers* **1963**, *1*, 545.
(37) Nutti, M. P.; de Bertoldi, M.; Lepidi, A. A. *Can. J. Microbiol.* **1972**, *18*, 1257.
(38) Dawes, E. A.; Senior, P. J. *Adv. Microbiol. Physiol.* **1973**, *10*, 135.
(39) Berger, E.; Ramsay, B. A.; Ramsay, J. A.; Chavarie, C.; Braunegg, G. *Biotechnol. Techniques 1989*, *3*, 4, 227.
(40) Ramsay, J. A.; Berger, E.; Ramsay, B. A.; Chavarie, C. *Biotechnol. Techniques* **1990**, *4*, 4, 221.
(41) Ramsay, J. A.; Berger, E.; Voyer, R.; Chavarie, C.; Ramsay, B. A. *Biotechnol. Techniques* **1994**, *8*, 8, 589.
(42) Ruel, K.; Ambert, K.; Joseleau, J.-P. *FEMS Microbiol. Rev.* **1994**, *13*, 241.
(43) Fraisse, D.; Schmitt, M. *Microchem. J.* **1977**, *22*, 109.
(44) Gagnon, K. D.; Fuller, R. C.; Lenz, R. W.; Farris, R. J. *Rubber World* **1992**, november, 32.
(45) Marchessault, R. H.; Monasterios, C. J.; Morin, F. G.; Sundararajan, P. R. *Int. J. Biol. Macromol.* **1990**, *12*, 158.

MA980508A